Coherent exciton-exciton interactions and exciton dynamics in a $MoSe_2/WSe_2$ heterostructure

Torben L. Purz,[1] Eric. W. Martin,[1,2] Pasqual Rivera,[3] William G. Holtzmann,[3] Xiaodong Xu,[3] and Steven T. Cundiff[1,*]

[1] *University of Michigan, Department of Physics, Ann Arbor, Michigan 48109, USA*
[2] *MONSTR Sense Technologies, LLC, Ann Arbor, Michigan 48104, USA*
[3] *Department of Physics, University of Washington, Seattle, Washington 98195-1560, USA*

(Dated: November 22, 2021)

Coherent coupling between excitons is at the heart of many-body interactions and quantum information with transition metal dichalcogenide (TMD) heterostructures as an emergent platform for the investigation of these interactions. We employ multi-dimensional coherent spectroscopy on monolayer $MoSe_2/WSe_2$ heterostructures and observe coherent coupling between excitons spatially localized in monolayer $MoSe_2$ and WSe_2. Through many-body spectroscopy, we further observe the absorption state arising from free interlayer electron-hole pairs. This observation yields a spectroscopic measurement of the interlayer exciton binding energy of about 250 meV.

Two-dimensional semiconducting transition metal dichalcogenides (TMDs) have received considerable attention in recent years for their efficient light-matter coupling, which has been harnessed in various optoelectronical applications [1–3]. Because of the high tunability of electronic properties, moiré superlattice effects for engineering interacting excitonic lattices [4, 5], and the strong Coulomb interactions at the 2D limit [6], they are an emergent platform for the investigation of many-body excitonic interactions. The strong Coulomb interactions yield strong coherent and incoherent interactions between different exciton states. Coherent coupling between excitons is crucial for many-body effects with potential applications such as electromagnetically induced transparency [7, 8], lasing without inversion [9–11] and excitonic quantum degenerate gases [12]. Furthermore, the interactions between excitons are important to understand for efficient opotoelectronic device design such as photovoltaics [13] and photodiodes [14]. Coherent coupling has already been observed in numerous conventional semiconductors [15–18] and recently in $MoSe_2$ monolayers [6, 19].

The coherent coupling between these quasiparticles also opens a new avenue for quantum information and quantum electronics applications with the electronic states of TMDs being easily accessible both optically and electronically. Quantum control of exciton qubits in quantum dots has been demonstrated in the past [20–22] and TMDs have been proposed as novel candidates for qubits via interlayer excitons [23], quantum dots [24] and defects [25] in TMD monolayers.

While for TMD heterostructures incoherent processes, including ultrafast charge transfer [26–32], the associated interlayer exciton formation [28, 31, 33–35], and energy transfer [27] have been extensively studied in the past, coherent coupling has been elusive in these samples due to the rapidness of the incoherent effects. Furthermore, the high binding energy of interlayer excitons in TMD heterostructures has raised interest in these excitons and their associated dynamics for excitonic integrated circuits and qubits [23, 33, 36]. In this letter, we employ multi-dimensional coherent spectroscopy (MDCS) to study coherent coupling dynamics and many-body effects for intra- and interlayer excitons in a $MoSe_2/WSe_2$ heterostructure. A simple scheme of MDCS is shown in Fig. 1(a).

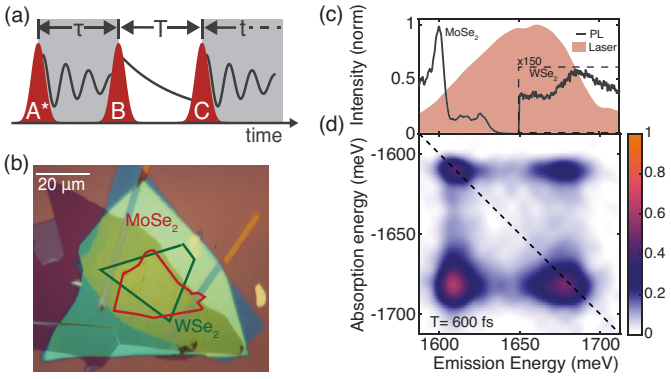

FIG. 1. (a) Schematic of a three-pulse MDCS experiment (Fourth pulse used for heterodyne detection not shown). (b) Microscope image of the heterostructure sample (c) Photoluminescence spectrum of the sample, together with the laser excitation spectrum. (d) Characteristic low-temperature, low-power multidimensional coherent spectrum of the $MoSe_2/WSe_2$ heterostructure at a pump-probe delay $T = 600$ fs. The occurence of two off-diagonal coupling peaks suggest the existence of coherent, and/or incoherent coupling channels between the two materials.

With MDCS, we measure the phase-resolved evolution of an induced nonlinear response. This response is induced by three pulses (A,B,C) impinging on the sample while a fourth pulse (not shown) is used for heterodyne detection. The four pulses are separated by time delays τ, T, and t. Recording the phase-resolved response along τ and t, and Fourier transforming yields (one-quantum) spectra correlating absorption and emission energies [37, 38], which is useful for measuring homogeneous and inhomogeneous linewidths, as well as many-

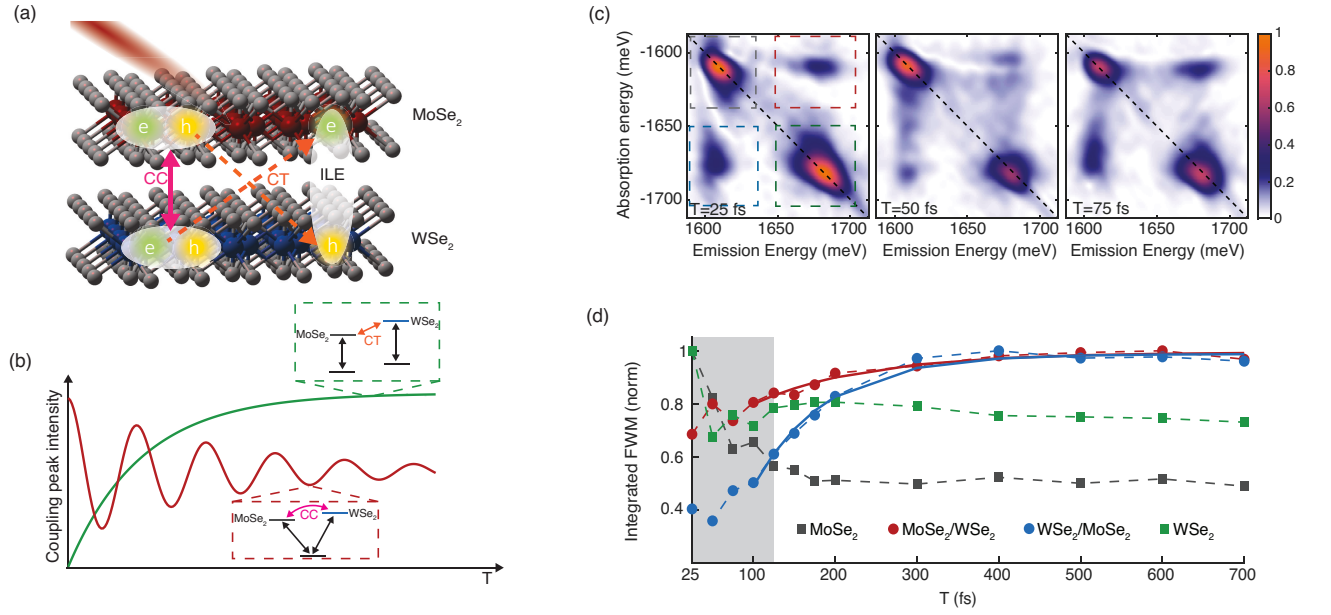

FIG. 2. (a) Illustration of coherently coupled $MoSe_2$ and WSe_2 excitons and the dephasing of coherent coupling (CC) via incoherent charge transfer (CT), yielding interlayer excitons (ILE) in the heterostructure. (b) Characteristic coupling peak amplitude dynamics and associated level-systems for incoherent vs. coherent coupling. (c) Characteristic low-temperature, low-power multidimensional coherent spectra of the $MoSe_2/WSe_2$ heterostructure at time-delays T=25 fs, T=50 fs, and T=75 fs. All spectra are plotted on the same color scale, shown for the spectrum taken at $T = 600$ fs in Fig. 1 (d). (d) Integrated four-wave mixing of the four peaks in the MDCS spectrum. Integration areas are marked by the dashed boxes in (c). Also shown are exponential fits to the rise behavior of the two coupling peaks from 100 fs on (solid lines).

body effects. Scanning the delay between the second and third pulse, T, reveals the temporal dynamics of the sample, similar to pump-probe, and distinguishes between coherent and incoherent coupling between different excitations [39]. For most of the results in this work we use these one-quantum spectra. For zero-quantum spectra we set $\tau = 0$ ps and move the T stage and perform a subsequent Fourier transform to obtain the mixing energy axis. Because the resonances in these heterostructure samples are very broad, even at the cryogenic temperatures and low powers used for the measurements in this work, we add up two different measurements: A one-quantum rephasing measurement, in which the first pump interaction is conjugate, and a one-quantum non-rephasing measurement where the second pump interaction is conjugate, generating absorptive spectra [39]. Adding these two measurements together allows us to further discern different effects within this heterostructure.

We cool the sample to a temperature of 5 K and use 100 fs pulses at an energy of 0.2 pJ/beam and a spot diameter of 1 μm to generate the third order response. Further technical details about the experiment can be found in the Supplemental Material [40].

A brightfield microscope image of the sample used in this work is provided in Fig. 1 (b). The sample consists of mechanically exfoliated $MoSe_2$ and WSe_2 monolayers stacked on top of each other with a near-zero twist angle. The heterostructure is encapsulated in hexagonal boron nitride (hBN). A photoluminescence (PL) spectrum for this heterostructure is shown in Fig. 1 (c). We also indicate the laser spectrum used in our experiment, which covers both the $MoSe_2$- and WSe_2-A exciton resonances. The MDCS spectrum in Fig. 1 (d), taken at $T = 600$ fs shows four peaks. The two peaks on the diagonal (dashed line) correspond to the resonance of the respective monolayers, while the two cross (or coupling) peaks with different absorption and emission energies are indicative of coupling between the two resonances. The spectral shift between features in PL and MDCS can be traced back to a combination of Stokes shift, spatial inhomogeneity, and limited bandwidth of the laser. From the roughly round shape of the on-diagonal peaks, we can deduce that the linewidths in this heterostructure sample are limited by the homogeneous linewidth. To confirm this conclusion, we fit cross-diagonal and on-diagonal slices [41] (Supplementary Information). From these fits we are able to extract the homogeneous linewidths for the two resonances, γ_{MoSe_2}=8.5 meV and γ_{WSe_2}=16.9 meV, which are an order of magnitude larger than for monolayer samples [42, 43]. It is reasonable to assume that this increase is due to additional population decay channels, such as charge transfer, in the heterostructure.

Discerning any other coupling between the excitons from the dominant charge transfer contribution is important. The key to this is the temporal evolution for the off-diagonal coupling peaks in the MDCS spectrum shown in Fig. 1 (d). There are two likely sources for the

occurence of these peaks:

1) After excitation by a laser, electrons and holes bind together to form excitons in the $MoSe_2$ and WSe_2 respectively, as shown in Fig. 2 (a). These excitons can coherently interact (coherent coupling), which can be caused by static dipole-dipole, exchange interactions, or transition dipole (Förster) coupling [44] among other things. This coupling manifests itself through an oscillating amplitude along T whose frequency matches the energy difference between the resonances as illustrated in Fig. 2(b). Decay of the oscillations stems from dephasing processes. This coupling can be thought of as a Raman-like nonradiative coherent superposition of the $MoSe_2$ and WSe_2 states during T, where the two states are coupled via a common ground state. In an ideal chirp free case, both coupling peaks oscillate in-phase. 2) Incoherent coupling channels, such as energy or charge transfer can also lead to an appearance of the coupling peaks. Charge transfer via electron and hole transfer as illustrated in Fig. 2(a), with subsequent formation of the interlayer exciton (ILE) is common in these TMD heterostructures. For this coupling, separate level systems do not need to share a common ground state in contrast to the coherent coupling, as illustrated in Fig. 2(b). Here, the coupling manifests iteself via a rise of the peak amplitude having a time scale characteristic of the transfer for these processes. An in-depth discussion of the different level systems can be found in the Supplemental Material [40].

To better resolve the dynamics of the heterostructure and determine the coupling mechanisms, we take several MDCS spectra with varying T delay. We show exemplary spectra taken at $T = 25$ fs, 50 fs, and 75 fs in Fig. 2 (c). The most notable changes between these spectra are a visible decay for the two on-diagonal peaks and varying amplitude for the coupling peaks. Overall, the coupling peak amplitude increases in time (compare Fig. 1 (d)). To better visualize these dynamics we integrate over each of the four peaks (integration area indicated by the dashed rectangles in Fig. 2 (c)), and plot the resulting integrated amplitudes in Fig. 2 (d). The decay of the on-diagonal peaks (squares) as well as the rise of the coupling peaks (circles) is clearly visible. Moreover, the amplitude of the two cross-peaks shows features suggestive of oscillations, a strong indication of coherent coupling. Coherent coupling also explains the significant non-zero amplitude of the two peaks at early times. The decay for both on-diagonal peaks occurs rapidly and noticeably faster than the rise of the coupling peaks. This decay can be explained by the multitude of processes, including rapid decay into dark or localized states as reported for both materials in the literature [43, 45] and population decay into the ground state, all of which affect the on-diagonal peaks. The rise of the coupling peaks, however, occurs only due to processes that incoherently couple the two materials together, such as energy and charge transfer. Based on the extensive literature on these heterostructures [26, 27, 29, 46] and the similar time-scale of the rise for the two coupling peaks, we deduce charge transfer to be the dominant incoherent coupling mechanism in this sample.

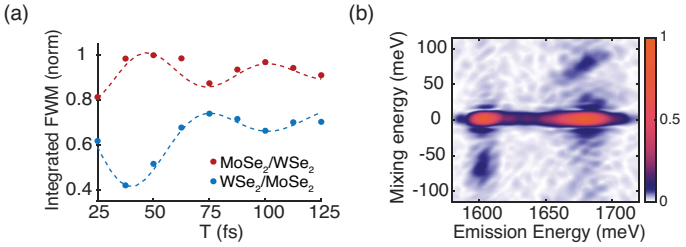

FIG. 3. (a) High temporal resolution measurement of the two-coupling peaks from Fig. 2(b). Curves have been offset to increase readability. The $MoSe_2/WSe_2$ curve was recorded with positive intentional GDD, the $WSe_2/MoSe_2$ curve was recorded with negative intentional GDD. (b) Zero-quantum spectrum, similar to Fourier-transforming with respect to the delay of a spectrally-resolved pump-probe experiment. Here, we added measurements taken with positive and negative intentional GDD. Complete data sets can be found in the Supplemental Material [40].

We fit an inverse exponential for $T \geq 100$ fs to the rise of the coupling peaks (solid lines) which yields an estimated rise time $\tau_{M\to W} < 149 \pm 28$ fs for the $MoSe_2/WSe_2$ peak and $\tau_{W\to M} < 91 \pm 9$ fs for the $WSe_2/MoSe_2$ peak, limited by the temporal resolution of 92 fs in our experiment (Supplementary Information). These values are in good agreement with the charge transfer times in the literature for similar samples [26, 27, 29, 46].

A separate data set with smaller T steps (range indicated by the gray area in Fig. 2 (d)), shown in Fig. 3 (a), resolves early time dynamics better. Both coupling peaks show clear oscillations with a frequency around $\hbar\omega = 74$ meV, corresponding to the energy difference between the $MoSe_2$ and WSe_2 excitons. These oscillations are emphasized by plotting a decaying cosine together with an exponential rise (dashed lines) as a guide to the eye. Since we see signatures of both coherent coupling and incoherent charge transfer, the resulting plots in Fig. 2(d) and Fig. 3(a) are the sum of a decaying oscillation and an exponential rise, as expected from Fig. 2(b).

A more quantitative measure of these oscillations can be obtained by taking a zero-quantum MDCS spectrum [47]. It is similar to spectrally-resolved pump-probe spectroscopy with an additional Fourier transform along the pump-probe delay T, which yields the mixing energy axis. Because we have used phase-resolved heterodyne detection, we can resolve the sign of the oscillation, which is different for the two coupling features in the zero-quantum spectrum shown in Fig. 3(b). The two features at zero mixing energy and $MoSe_2$ or WSe_2 emission energy correspond to the non-oscillating contributions of both on-diagonal and coupling peaks. Two features around a mixing energy of +71 meV and -74 meV can be seen for the $MoSe_2$ and WSe_2 emission, respectively. Within the sample inhomogeneity, this matches the energy spacing between the $MoSe_2$ and WSe_2-A ex-

citons. This agreement supports the fact that excitons in the two materials are indeed coherently coupled and oscillate during T with a frequency determined by the energy difference of the two resonances. The broadness of the features stems from the fact that both coupling contributions decay rapidly along T. The low energy (10-20 meV) signatures are due to truncation effects. The nature of the coherent coupling is not immediately evident and needs further investigation. Common interactions that lead to coherent coupling are biexcitonic of nature, such as static dipole-dipole or exchange interactions, or due to mixing of the single exciton states, such as transition dipole (Förster) coupling [44, 48]. They can, for example, be distinguished by careful analysis of the real part of the MDCS spectrum, as demonstrated in [44]. Future experiments using double-quantum coherent spectroscopy can also provide insight into the nature of the coherent coupling [15, 16]. In the current stage, the rapid dephasing of coherent coupling due to the rapid dephasing of the excitons, which itself is caused by the rapid charge transfer, limits applications of coherent coupling in these samples, and further work is required to transform this into viable applications. In Fig. 3 (a) and (b), we combine measurements with intentional small negative and positive group-delay dispersion (GDD) on the three excitation pulses, which enhances the coherent oscillations that are otherwise obscured by residual third order dispersion. The time resolution for incoherent and coherent dynamics are essentially different: While the incoherent dynamics are limited by the chirped pulse, the measurement of the coherent processes, in theory, is not affected by chirp and given by the transform limited pulse. However, there are intricacies with regards to dephasing as discussed in the Supplementary Information [40], that render efficient dispersion control a necessity for the observation of coherent coupling.

We furthermore acquired MDCS spectra with varying T delay over an intermediate (500 fs-5 ps) to longterm (150 ps-600 ps) time range, whose integrated peak amplitudes are shown in Fig. 4 (a), starting at 500 fs, after the initial coupling peak rise and on-diagonal peak decay. The full dataset can be found in the Supplementary Information.

Within the first 5 ps, three of the four peaks (except the $MoSe_2$ peak) decay, followed by another decay for all four peaks for $T \geq 100$ ps. This behavior is consistent with the literature, which reports bi-exponential time-scales in the intermediate and long term dynamics of these samples [28, 29, 31]. In contrast to previous experiments however, which look at the coupling dynamics in an isolated setting, the MDCS approach reveals distinctly different decay constants for the four peaks, hinting at superposition of dynamics that cannot be obtained in the selective experiments in the literature. In the intermediate time frame, the $MoSe_2/WSe_2$ peak (τ=1.22±0.12 ps), as well as the WSe_2 peak (τ=1.51±0.12 ps) decay quicker and with a larger amplitude than the $WSe_2/MoSe_2$ peak (τ=1.69±0.16 ps) and $MoSe_2$ peak (no fit). Here, τ denotes the decay constant from a simple exponential decay. Competition between several dynamical processes can explain this surprising behavior. We attribute the initial decay of the coupling peaks to the phonon-assisted relaxation of momentum-space "hot" interlayer excitons [33] into a tightly bound interlayer exciton state. Either the difference in many-body effects of the hot vs. tightly bound interlayer excitons, or the fact that the hot interlayer excitons are more prone to electron-hole recombination than their tightly bound counterparts can explain an initial decay of the coupling peaks, because both processes would indirectly affect the intralayer excitons and thus the coupling peak strength. The difference in decay between the $MoSe_2$ and WSe_2 during the first 5 ps warrants further study. The likely explanation is energy transfer from WSe_2 into the $MoSe_2$ that contributes on these intermediate time-scales [27].

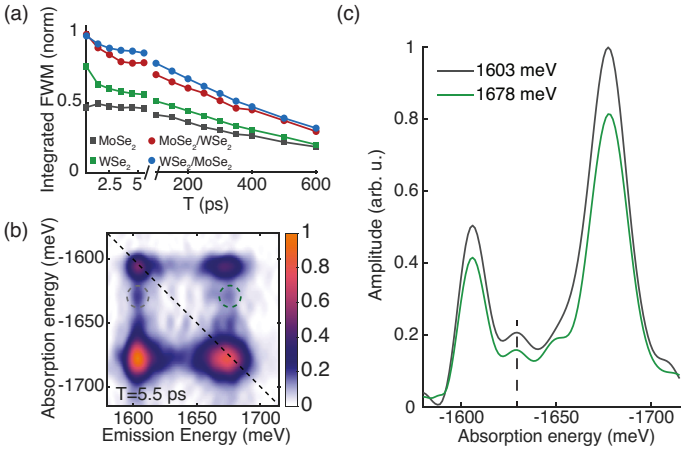

FIG. 4. (a) Integrated four-wave mixing of the four peaks in the MDCS spectrum for intermediate and long times (500 fs-600 ps). (b) Characteristic low-temperature, low-power multidimensional coherent spectrum of the $MoSe_2/WSe_2$ heterostructure at a pump-probe time-delay of T=5.5 ps. (c) Slices of fixed emission energy taken along the absorbtion energy axis. The dashed line indicates the absorption energy for the interlayer exciton feature.

The long term decay, which is fitted separately due to competing dynamics at early times, shows a roughly uniform timescale for all four peaks (607 ± 22 ps, 580 ± 28 ps, 540 ± 8 ps ,520 ± 13 ps from left to right, top to bottom) within the uncertainty of the measurement and noise. We attribute this decay to interlayer exciton decay. The literature has reported interlayer exciton lifetimes from hundreds of picoseconds, to hundreds of nanoseconds, depending on the twist angle and other sample parameters [34, 49–52], with [53] reporting a decay time of 1.3 ns for a 1° twist angle, increasing by more than an order of magnitude for a 3.5° twist angle. Given the near zero-twist angle of the sample studied in this report and common sample-to-sample variations, our values are in good agreement with these findings.

We have reproduced all the dynamics in this sample,

including charge transfer, coherent coupling, and hot interlayer exciton relaxation in a similar $MoSe_2/WSe_2$ heterostructure (Supplementary Information), showing that the occurence of these dynamics is not sample specific.

After the relaxation of the hot interlayer excitons, another signature of the interlayer exciton is obtained in the MDCS spectra. An MDCS spectrum with a T delay of 5.5 ps is shown in Fig. 4 (b). The features that show absorption at continuum energies around 1629 meV and emission at the $MoSe_2$ and WSe_2-A exciton resonances (dashed circles), have no visible corresponding on-diagonal peaks, and no emission at comparable energies. Therefore these spectral features cannot be due to another material resonance. Instead, we believe that this features occurs due to the continuum absorption generating free interlayer electron/hole pairs, which subsequently affect the emission of the $MoSe_2$ and WSe_2 excitons via many-body effects. The weak absorption by the free interlayer electron-hole pairs is compensated by their very strong Coulomb interaction with the excitons. Similar effects have been observed in GaAs quantum wells [48, 54]. Two slices, taken at fixed emission energies of 1603 meV and 1678 meV along the absorption energy axis are displayed in Fig. 4 (c). From this, we determine the interlayer exciton absorption feature to be at 1629 meV. From our PL measurement, the ILE emission is known to be at 1.375 eV (Supplementary Information). From the difference between these energies we deduce the binding energy of the interlayer excitons in this sample to be around 254 meV. This is in excellent agreement with a recently performed first principle calculation [35], which estimates the binding energy to be around 250 meV, and above other theoretically predicted values [55]. This binding energy is consistent with previously measured binding energies in these samples at 110 K using microARPES and PL [56], and two times larger than measured binding energies in a WSe_2/WS_2 heterostructure [33].

In summary, we demonstrated coherent exciton-exciton coupling, rapid charge transfer, and tightly bound interlayer excitons with binding energies above 200 meV on a mixed TMD heterostructure. These results underscore the immense technological potential for these materials. Studying the nature of the coherent coupling as well as how to tune it will remain an exciting challenge for future work.

We thank M.W. Day for fruitful discussion. The research at U. of Michigan was supported by NSF Grant No. 2016356. The work at U. Washington was supported by the Department of Energy, Basic Energy Sciences, Materials Sciences and Engineering Division (DE-SC0018171). W.G.H. was supported by the NSF Graduate Research Fellowship Program under Grant No. DGE-1762114.

* cundiff@umich.edu

[1] A. Pospischil, M. Furchi, and T. Mueller, Solar-energy conversion and light emission in an atomic monolayer p–n diode, Nature Photonics **9**, 257–261 (2014).

[2] Z. Ye, Y.and Wong and X. Lu, Monolayer excitonic laser, Nature Photonics **9**, 733–737 (2015).

[3] K. Mak and J. Shan, Photonics and optoelectronics of 2D semiconductor transition metal dichalcogenides, Nature Photon **10**, 216 (2016).

[4] K. L. Seyler, P. Rivera, H. Yu, N. P. Wilson, E. L. Ray, D. G. Mandrus, J. Yan, W. Yao, and X. Xu, Signatures of moiré-trapped valley excitons in Mose2/Wse2 heterobilayers, Nature **567**, 66 (2019).

[5] H. Yu, G.-B. Liu, J. Tang, X. Xu, and W. Yao, Moiré excitons: From programmable quantum emitter arrays to spin-orbit–coupled artificial lattices, Science Advances **3**, 10.1126/sciadv.1701696 (2017).

[6] K. Hao, L. Xu, P. Nagler, A. Singh, K. Tran, C. K. Dass, C. Schüller, T. Korn, X. Li, and G. Moody, Coherent and incoherent coupling dynamics between neutral and charged excitons in monolayer $MoSe_2$, Nano Letters **16**, 5109 (2016), pMID: 27428509, https://doi.org/10.1021/acs.nanolett.6b02041.

[7] K.-J. Boller, A. Imamoğlu, and S. E. Harris, Observation of electromagnetically induced transparency, Phys. Rev. Lett. **66**, 2593 (1991).

[8] J. E. Field, K. H. Hahn, and S. E. Harris, Observation of electromagnetically induced transparency in collisionally broadened lead vapor, Phys. Rev. Lett. **67**, 3062 (1991).

[9] S. E. Harris, Lasers without inversion: Interference of lifetime-broadened resonances, Phys. Rev. Lett. **62**, 1033 (1989).

[10] M. O. Scully, S.-Y. Zhu, and A. Gavrielides, Degenerate quantum-beat laser: Lasing without inversion and inversion without lasing, Phys. Rev. Lett. **62**, 2813 (1989).

[11] A. S. Zibrov, M. D. Lukin, D. E. Nikonov, L. Hollberg, M. O. Scully, V. L. Velichansky, and H. G. Robinson, Experimental demonstration of laser oscillation without population inversion via quantum interference in Rb, Phys. Rev. Lett. **75**, 1499 (1995).

[12] M. Combescot, R. Combescot, and F. Dubin, Bose–einstein condensation and indirect excitons: a review, Reports on Progress in Physics **80**, 066501 (2017).

[13] N. Flöry, A. Jain, P. Bharadwaj, M. Parzefall, T. Taniguchi, K. Watanabe, and L. Novotny, A $WSe_2/MoSe_2$ heterostructure photovoltaic device, Applied Physics Letters **107**, 123106 (2015), https://doi.org/10.1063/1.4931621.

[14] J. E. Kim, W. T. Kang, V. Tu Vu, Y. R. Kim, Y. S. Shin, I. Lee, U. Y. Won, B. H. Lee, K. Kim, T. L. Phan, Y. H. Lee, and W. J. Yu, Ideal pn photodiode using doping controlled WSe_2-$MoSe_2$ lateral heterostructure, J. Mater. Chem. C **9**, 3504 (2021).

[15] G. Nardin, G. Moody, R. Singh, T. M. Autry, H. Li, F. Morier-Genoud, and S. T. Cundiff, Coherent excitonic coupling in an asymmetric double InGaAs quantum well arises from many-body effects, Phys. Rev. Lett.

112, 046402 (2014).
[16] G. Moody, I. A. Akimov, H. Li, R. Singh, D. R. Yakovlev, G. Karczewski, M. Wiater, T. Wojtowicz, M. Bayer, and S. T. Cundiff, Coherent coupling of excitons and trions in a photoexcited CdTeCdMgTe quantum well, Phys. Rev. Lett. **112**, 097401 (2014).
[17] E. Harel, S. M. Rupich, R. D. Schaller, D. V. Talapin, and G. S. Engel, Measurement of electronic splitting in PbS quantum dots by two-dimensional nonlinear spectroscopy, Phys. Rev. B **86**, 075412 (2012).
[18] P. Borri and W. Langbein, Four-wave mixing dynamics of excitons in InGaAs self-assembled quantum dots, Journal of Physics: Condensed Matter **19**, 295201 (2007).
[19] A. Singh, G. Moody, S. Wu, Y. Wu, N. J. Ghimire, J. Yan, D. G. Mandrus, X. Xu, and X. Li, Coherent electronic coupling in atomically thin $MoSe_2$, Phys. Rev. Lett. **112**, 216804 (2014).
[20] D. Press, T. D. Ladd, B. Zhang, , and Y. Yamamoto, Complete quantum control of a single quantum dot spin using ultrafast optical pulses, Nature **456**, 218–221 (2008).
[21] J. Berezovsky, M. H. Mikkelsen, N. G. Stoltz, L. A. Coldren, and D. D. Awschalom, Picosecond coherent optical manipulation of a single electron spin in a quantum dot, Science **320**, 349 (2008).
[22] M. Koch, J. Feldmann, G. von Plessen, E. O. Göbel, P. Thomas, and K. Köhler, Quantum beats versus polarization interference: An experimental distinction, Phys. Rev. Lett. **69**, 3631 (1992).
[23] S. Miao, T. Wang, X. Huang, D. Chen, Z. Lian, C. Wang, M. Blei, T. Taniguchi, K. Watanabe, S. Tongay, Z. Wang, D. Xiao, Y.-T. Cui, and S.-F. Shi, Strong interaction between interlayer excitons and correlated electrons in WSe2/WS2 moiré superlattice, Nat Commun **12**, 10.1038/s41467-021-23732-6 (2021).
[24] J. Pawłowski, M. Bieniek, and T. Wozniak, Valley two-qubit system in a MoS_2-monolayer gated double quantum dot, Phys. Rev. Applied **15**, 054025 (2021).
[25] P. M. M. de Melo, P. Miguel, Z. Zanolli, and M. J. Verstraete, Optical signatures of defect centers in transition metal dichalcogenide monolayers, Advanced Quantum Technologies **4**, 2000118 (2021).
[26] Hong, Xiaoping and Kim, Jonghwan and Shi, Su-Fei and Zhu Yu, and Jin Chenhao and Sun Yinghui annd Tongay, Sefaattin and Wu, Junqiao and Zhang, Yanfeng and Wang, Feng, Ultrafast charge transfer in atomically thin MoS_2/WS_2 heterostructures, Nature Nanotech , 682–686 (2014).
[27] D. Kozawa, A. Carvalho, I. Verzhbitskiy, F. Giustiniano, Y. Miyauchi, S. Mouri, A. H. Castro Neto, K. Matsuda, and G. Eda, Evidence for fast interlayer energy transfer in $MoSe_2/WS_2$ heterostructures, Nano Letters **16**, 4087 (2016).
[28] H. Chen, X. Wen, J. Zhang, T. Wu, Y. Gong, X. Zhang, J. Yuan, C. Yi, J. Lou, P. M. Ajayan, W. Zhuang, G. Zhang, and J. Zheng, Ultrafast formation of interlayer hot excitons in atomically thin MoS_2/WS_2 heterostructures, Nat Commun **7**, 12512 (2016).
[29] J. E. Zimmermann, Y. D. Kim, J. C. Hone, U. Höfer, and G. Mette, Directional ultrafast charge transfer in a $WSe_2/MoSe_2$ heterostructure selectively probed by time-resolved shg imaging microscopy, Nanoscale Horiz. **5**, 1603 (2020).
[30] S. Ovesen, S. Brem, C. Linderälv, M. Kuisma, T. Korn, P. Erhart, M. Selig, and E. Malic, Interlayer exciton dynamics in van der waals heterostructures, Commun Phys **2**, 10.1038/s42005-019-0122-z (2019).
[31] J. Liu, X. Zhang, and G. Lu, Excitonic effect drives ultrafast dynamics in van der waals heterostructures, Nano Letters **20**, 4631 (2020), pMID: 32432887, https://doi.org/10.1021/acs.nanolett.0c01519.
[32] V. R. Policht, M. Russo, F. Liu, C. Trovatello, M. Maiuri, Y. Bai, X. Zhu, S. Dal Conte, and G. Cerullo, Dissecting interlayer hole and electron transfer in transition metal dichalcogenide heterostructures via two-dimensional electronic spectroscopy, Nano Letters **21**, 4738 (2021), pMID: 34037406, https://doi.org/10.1021/acs.nanolett.1c01098.
[33] Merkl, P. and Mooshammer, F. and Steinleitner, P. and Girnghuber, A. and Lin, K.-Q., and Nagler, P. and Holler, J. and Schüller, C. and Lupton, J.M. and Korn, T. and Ovesen, S. and Brem, S. and Malic, E. and Huber, E., Ultrafast transition between exciton phases in van der waals heterostructures, Nat. Mater. **18**, 691–696 (2019).
[34] P. Rivera, J. Schaibley, A. Jones, J. Ross, S. Wu, G. Aivazian, P. Klement, K. Seyler, G. Clark, N. Ghimire, J. Yan, D. Mandrus, W. Yao, and X. Xu, Observation of long-lived interlayer excitons in monolayer $MoSe_2$-WSe_2 heterostructures, Nat Commun **6**, 6242 (2015).
[35] R. Gillen and J. Maultzsch, Interlayer excitons in $MoSe_2/WSe_2$ heterostructures from first principles, Phys. Rev. B **97**, 165306 (2018).
[36] Y. Jiang, S. Chen, W. Zheng, B. Zheng, and A. Pan, Interlayer exciton formation, relaxation, and transport in tmd van der waals heterostructures, Light Sci Appl **10**, 10.1038/s41377-021-00500-1 (2021).
[37] S. Cundiff and S. Mukamel, Optical multidimensional coherent spectroscopy, Phys. Today **44**, 10.1063/PT.3.2047 (2013).
[38] E. W. Martin and S. T. Cundiff, Inducing coherent quantum dot interactions, Phys. Rev. B , 081301 (2018).
[39] C. L. Smallwood and S. T. Cundiff, Multidimensional coherent spectroscopy of semiconductors, Laser & Photonics Reviews **12**, 1800171 (2018).
[40] See Supplemental Material at [URL will be inserted by publisher] for details of the experiment and simulation as well as supplemental data which includes Refs. [57–59].
[41] M. E. Siemens, G. Moody, H. Li, A. D. Bristow, and S. T. Cundiff, Resonance lineshapes in two-dimensional faourier transform spectroscopy, Opt. Express **18**, 17699 (2010).
[42] E. W. Martin, J. Horng, H. G. Ruth, E. Paik, M.-H. Wentzel, H. Deng, and S. T. Cundiff, Encapsulation narrows and preserves the excitonic homogeneous linewidth of exfoliated monolayer $MoSe_2$, Phys. Rev. Applied **14**, 021002 (2020).
[43] G. Moody, C. Kavir Dass, K. Hao, C.-H. Chen, L.-J. Li, A. Singh, K. Tran, G. Clark, G. Xu, Xiaodong and-Berghäuser, E. Malic, A. Knorr, and X. Li, Intrinsic homogeneous linewidth and broadening mechanisms of excitons in monolayer transition metal dichalcogenides, Nat Commun **6**, 8315 (2015).
[44] B. Kasprzak, J.and Patton, V. Savona, and W. Langbein, Coherent coupling between distant excitons revealed by two-dimensional nonlinear hyperspectral imaging, Nature Photonics , 57–63 (2011).
[45] T. Jakubczyk, V. Delmonte, M. Koperski, K. Noga-

jewski, C. Faugeras, W. Langbein, M. Potemski, and J. Kasprzak, Radiatively limited dephasing and exciton dynamics in $MoSe_2$ monolayers revealed with four-wave mixing microscopy, Nano Letters **16**, 5333 (2016).

[46] B. Peng, G. Yu, X. Liu, B. Liu, X. Liang, L. Bi, L. Deng, T. C. Sum, and K. P. Loh, Ultrafast charge transfer in MoS_2/WS_2 p–n heterojunction, 2D Materials **3**, 025020 (2016).

[47] L. Yang, T. Zhang, A. D. Bristow, S. T. Cundiff, and S. Mukamel, Isolating excitonic raman coherence in semiconductors using two-dimensional correlation spectroscopy, The Journal of Chemical Physics **129**, 234711 (2008), https://doi.org/10.1063/1.3037217.

[48] T. Zhang, I. Kuznetsova, T. Meier, X. Li, R. P. Mirin, P. Thomas, and S. T. Cundiff, Polarization-dependent optical 2D fourier transform spectroscopy of semiconductors, Proceedings of the National Academy of Sciences **104**, 14227 (2007), https://www.pnas.org/content/104/36/14227.full.pdf.

[49] J. Choi, M. Florian, A. Steinhoff, D. Erben, K. Tran, D. S. Kim, L. Sun, J. Quan, R. Claassen, S. Majumder, J. A. Hollingsworth, T. Taniguchi, K. Watanabe, K. Ueno, A. Singh, G. Moody, F. Jahnke, and X. Li, Twist angle-dependent interlayer exciton lifetimes in van der waals heterostructures, Phys. Rev. Lett. **126**, 047401 (2021).

[50] C. Choi, J. Huang, H.-C. Cheng, H. Kim, A. K. Vinod, S.-H. Bae, V. O. Özcelik, R. Grassi, J. Chae, S.-W. Huang, X. Duan, K. Kaasbjerg, T. Low, and C. W. Wong, Enhanced interlayer neutral excitons and trions in trilayer van der waals heterostructures, npj 2D Mater Appl **2**, 30 (2018).

[51] M. Baranowski, A. Surrente, L. Klopotowski, J. M. Urban, N. Zhang, D. K. Maude, K. Wiwatowski, S. Mackowski, Y. C. Kung, D. Dumcenco, A. Kis, and P. Plochocka, Probing the interlayer exciton physics in a $MoS_2/MoSe_2/MoS_2$ van der waals heterostructure, Nano Letters **17**, 6360 (2017), pMID: 28895745, https://doi.org/10.1021/acs.nanolett.7b03184.

[52] B. Miller, A. Steinhoff, B. Pano, J. Klein, F. Jahnke, A. Holleitner, and U. Wurstbauer, Long-lived direct and indirect interlayer excitons in van der waals heterostructures, Nano Letters **17**, 5229 (2017), pMID: 28742367, https://doi.org/10.1021/acs.nanolett.7b01304.

[53] J. Choi, M. Florian, A. Steinhoff, D. Erben, K. Tran, D. S. Kim, L. Sun, J. Quan, R. Claassen, S. Majumder, J. A. Hollingsworth, T. Taniguchi, K. Watanabe, K. Ueno, A. Singh, G. Moody, F. Jahnke, and X. Li, Twist angle-dependent interlayer exciton lifetimes in van der waals heterostructures, Phys. Rev. Lett. **126**, 047401 (2021).

[54] C. N. Borca, T. Zhang, X. Li, and S. T. Cundiff, Optical two-dimensional fourier transform spectroscopy of semiconductors, Chemical Physics Letters **416**, 311 (2005).

[55] S. Ovesen, S. Brem, C. Linderaelv, M. Kuisma, T. Korn, P. Erhart, M. Selig, and E. Malic, Interlayer exciton dynamics in van der waals heterostructures, Communications Physics **2**, doi.org/10.1038/s42005-019-0122-z (2019).

[56] N. R. Wilson, P. V. Nguyen, K. Seyler, P. Rivera, A. J. Marsden, Z. P. L. Laker, G. C. Constantinescu, V. Kandyba, A. Barinov, N. D. M. Hine, X. Xu, and D. H. Cobden, Determination of band offsets, hybridization, and exciton binding in 2d semiconductor heterostructures, Science Advances **3**, 10.1126/sciadv.1601832 (2017).

[57] D. Polli, D. Brida, S. Mukamel, G. Lanzani, and G. Cerullo, Effective temporal resolution in pump-probe spectroscopy with strongly chirped pulses, Phys. Rev. A **82**, 053809 (2010).

[58] P. F. Tekavec, J. A. Myers, K. L. M. Lewis, F. D. Fuller, and J. P. Ogilvie, Effects of chirp on two-dimensional fourier transform electronic spectra, Opt. Express **18**, 11015 (2010).

[59] P. Hamm and M. Zanni, *Concepts and Methods of 2D Infrared Spectroscopy* (Cambridge University Press, 2011).